

The Effect of Re, S, and Cl on the Deactivation of Pt/ γ -Al₂O₃ Reforming Catalysts

S. M. AUGUSTINE, G. N. ALAMEDDIN, AND W. M. H. SACTLER

Ipatieff Laboratory, Center for Catalysis and Surface Science, Departments of Chemistry and Chemical Engineering, Northwestern University, Evanston, Illinois 60208

Received July 8, 1988; revised August 12, 1988

The effects upon *n*-hexane (*n*C₆) conversion and catalyst deactivation caused by adding Re, S, and Cl to Pt/Al₂O₃, and also by varying the Pt and Re interaction, were studied. The *n*C₆ reaction was studied at atmospheric pressure, 400°C, and H₂/*n*C₆ = 9. The amount of carbon and hydrogen deposited on the catalyst during reaction was determined by temperature-programmed oxidation with an on-line mass spectrometer. Re addition to Pt/Al₂O₃ increases the rate of deactivation, but lowers the amount of C retained on the catalyst. S addition increases activity maintenance, in addition to lowering the amount of C. Most remarkably, the H/C ratio of the carbonaceous layer is much higher for presulfided samples. Cl⁻ increases the amount on the support relative to that on the metal. The results are consistent with a model assuming that S is preferentially chemisorbed on Re sites in bimetallic PtRe particles. This S divides the PtRe surface into small Pt ensembles. Consequently, hydrogenolysis activity is suppressed, and reorganization of carbonaceous overlayers into pseudo-graphitic entities that are detrimental to catalytic activity is impeded. © 1989 Academic Press, Inc.

A. INTRODUCTION

Catalysis of hydrocarbon conversion over PtRe/ γ -Al₂O₃ catalysts has been the subject of numerous papers and patents, since Kluksdahl (1) revealed the superior performance of this system in catalytic reforming. Bertolacini and Pellet (2) emphasized that the main advantage of the Re-containing catalyst over the conventional reforming catalyst was the superior *activity maintenance*, which could even be obtained by starting from a physical mixture of alumina-supported Pt and Re compounds. Bolivar *et al.* (3) also studied physical mixtures and found for α -Al₂O₃-supported samples that the surface mobility of the Re precursor over the alumina surface is significant; after reduction Re was detected on those support particles that initially contained only Pt. In our own work (4, 5) with γ -Al₂O₃-supported samples it was found that the surface migration of the Re precursor can be controlled by chemical treatments; high mobility results in both a

distinct lowering of the TPR peak temperature for Re and a significant increase in the TOF for cyclopentane hydrogenolysis, a reaction which is very specific for mixed PtRe surface ensembles.

This high hydrogenolysis activity of PtRe clusters, converting hydrocarbons largely to methane, which had been first reported by Haining *et al.* (6), shows that pure PtRe clusters or "alloy" particles are obviously *not* the active ingredients of the technical naphtha reforming catalysts. The model for the superior activity maintenance, which was proposed first in 1980 by Biloen *et al.* (7), therefore accepts that under actual industrial conditions the catalyst is exposed to traces of sulfur-containing compounds, either during conditioning or during the process proper. In view of the high chemical affinity of Re for sulfur it is, therefore, assumed that in the steady state the catalyst contains PtRe clusters on the alumina, and sulfur atoms are preferentially adsorbed onto Re atoms of the surface of these clusters. This model was further elaborated by

Sachtler (8) who considered the nature of catalyst deactivation by pseudo-graphitic or "hard" coke. Somorjai and Blakeley (9) had shown that the reorganization of hydrocarbonaceous overlayers to more harmful species distinctly depends on the topography of the adsorbing metal surface; flat surfaces are more easily covered than stepped surfaces. Lankhorst *et al.* further demonstrated an effect of platinum particle size (10). Sedentary hydrocarbon fragments CH_x , with x near 2, probably pose only a mild hazard if any, to catalyst activity (11). Some researchers actually credit this "soft coke" with promoter properties, transferring hydrogen from the metal surface to chemisorbed molecules and providing sites for product desorption (12–14). Under steady-state conditions, the deactivation of industrial PtRe catalysts will then be controlled by loss of hydrogen and a reorganization of the omnipresent hydrocarbonaceous overlayer to (pseudo-)graphitic entities covering the metal particles. Such "hard coke" is not revolatilized under the steady-state conditions of catalytic reforming. In view of the topological effects in this reconstruction, Sachtler speculated that strongly chemisorbed sulfur atoms might form an efficient obstacle against this reorganization of "soft coke" to "hard coke," which would explain why alumina-supported PtRe–S particles display such an enhanced activity maintenance.

This model was examined in further work by systematically comparing activity, selectivity of hydrocarbon conversion, and their dependence on time on stream, both at atmospheric (15) and at elevated pressure (16). All results confirmed the crucial role of traces of sulfur in transforming PtRe/ γ - Al_2O_3 preparations into catalysts of low hydrogenolysis selectivity, but excellent activity maintenance. While these results lend credence to the above model, direct evidence that the presence of adsorbed sulfur alters the nature of the carbonaceous overlayer which is formed on the catalyst as a by-product of hydrocarbon

conversion is lacking. The objective of the present work is to obtain such evidence. Various supported Pt and PtRe preparations were used as catalysts in a simple hydrocarbon conversion test under standardized conditions; the samples were then subjected to temperature-programmed oxidation (TPO) to analyze the (hydro-)carbonaceous overlayer. The latter procedure is similar to that used by Barbier *et al.* (17). An oxygen-containing gas is led over the sample; while its temperature is increased in a programmed manner, the consumption of oxygen and the formation of carbon dioxide are registered continuously by on-line mass spectrometry. The spectra show peaks which are attributed to the oxidation of the hydrocarbonaceous overlayers on the metal and the support, respectively. Subsequent TPR shows that the metals are completely oxidized during TPO runs. Therefore, the distribution of the total oxygen consumption over the three components is calculated: C atoms are oxidized to CO_2 , H atoms to H_2O and metal atoms to PtO_2 and Re_2O_7 .

Various authors have published data on temperature-programmed oxidation of carbonaceous overlayers. Unfortunately often an "accelerated coking" procedure has been used (18–21), where a very low hydrogen pressure is maintained during coke deposition. Under these conditions diene formation is likely to be significant, which led some authors to assume that catalyst deactivation be due to dehydrogenation over the metal function (18–22), although it is widely accepted that the metal function hydrogenates coke precursors produced on the acidic support (23). In addition, it is debatable whether carbonaceous overlayers produced at extremely low hydrogen/hydrocarbon ratios can be characteristic for the "coke" formed under actual hydrocarbon conversion catalysis. Therefore, we decided to test samples under somewhat more realistic conditions, although using model compounds and atmospheric pressure. Our characterization of the "coke" layer is fo-

cused on the quantity (C/M ratio), location (peak position), and composition (H/C ratios) of the overlayer. The catalyst parameters under consideration are (i) metal function (Pt or Re) isolated on a nonacidic SiO₂ or NaY support, (ii) Lewis acidity of the support (partially dehydroxylated γ -Al₂O₃), (iii) bimetallic versus monometallic catalysts, (iv) addition of sulfur, (v) alteration of Pt and Re interaction by changing catalyst preparation, and (vi) Cl⁻ addition as a possible means of increasing the Brønsted acidity of the support.

B. EXPERIMENTAL

B1. Catalyst Preparation

All catalysts supported on nonchlorided alumina are prepared by incipient wetness impregnation onto Cyanamid PHF γ -Al₂O₃ (surface area 180 m²/g; pore volume 0.5 cm³/g; mesh size 60–80). Solutions of Pt(NH₃)₄(NO₃)₂ and NH₄ReO₄ in doubly distilled water are used for impregnation. In the case of the alumina-supported bimetallic catalyst, coimpregnation makes use of a solution containing both the Pt and the Re compounds. After impregnation, the catalysts are dried at 120°C in an oven overnight, calcined at 500°C in flowing dry air for 2 h, and stored in bottles before use. The final loading of the catalysts are 0.35 wt% Pt/Al₂O₃, 0.20 wt% Re/Al₂O₃, and 0.33 wt% Pt–0.22 wt% Re/Al₂O₃, as determined by atomic absorption at Galbraith Labs. A 1.0 wt% Pt/SiO₂ and a 0.87 wt% Re/SiO₂ were prepared in a similar manner with Davison Grade 62 SiO₂ as the support.

We also make use of a second preparation method in which the amount of Pt and Re interaction is varied. This method starts with impregnation of Pt onto γ -Al₂O₃ followed by calcination as above and reduction in flowing hydrogen at 500°C. The sample is then impregnated with NH₄ReO₄, dried overnight at 120°C, and allowed to pick up moisture from the atmosphere for 1 week at room temperature. The purpose of this is to avoid any high-temperature calci-

nation step with supported Re prior to catalyst *in situ* treatments. As reported earlier, catalyst calcination at elevated temperatures, prior to reduction, immobilizes the Re precursor and leads to little interaction of Pt and Re in the reduced catalyst. Rhenium migration is much more extensive if the catalysts are directly reduced without being subjected to high temperatures (5). The metal loading is 0.18 wt% Pt–0.41 wt% Re/Al₂O₃. This preparation will be referred to by the term "successive impregnation," and the catalyst will be designated "PtRe/Al₂O₃(SI)."

The Pt/Al₂O₃–Cl and PtRe/Al₂O₃–Cl catalysts used in this study were prepared by American Cyanamid. The metal loadings of these catalysts are 0.71 wt% Pt, for the monometallic sample, and 0.39 wt% Pt–0.41 wt% Re for the bimetallic sample. There was about 1 wt% Cl in every catalyst.

A NaY-supported Pt catalyst was also studied. Its preparation is described elsewhere (24). The metal loadings as well as the dispersions of the catalysts, as determined by H/D titrations (25), are listed in Table 1.

The gases used in this study were supplied by Matheson and are U.H.P. grade. Pretreatment consists of passing the O₂/He mixture over a Pt/SiO₂ trap to remove any H₂; all other gases are passed through an

TABLE I
Loadings and Dispersions of Catalysts

Catalysts	wt% Pt	wt% Re	H/M
Pt/NaY	2.4	—	1.0
Pt/SiO ₂	0.49	—	0.67
Re/SiO ₂	—	0.89	NA
Pt/Al ₂ O ₃	0.35	—	0.91
Re/Al ₂ O ₃	—	0.20	0.68
PtRe/Al ₂ O ₃	0.33	0.22	0.70
Pt/Al ₂ O ₃ –Cl	0.71	—	0.67
PtRe/Al ₂ O ₃ –Cl	0.39	0.44	0.49
PtRe/Al ₂ O ₃ (SI)	0.18	0.41	
No pretreatment			0.69
Ar, 500°C			0.93

MnO trap to remove O₂. All gases are then passed over a 4-Å molecular sieve at -78°C to trap H₂O. The H₂S/H₂ consists of 9.4 ppm H₂S in H₂ as analyzed by Matheson prior to shipping. The H₂S mixture is used without further treatment.

B2. Catalytic Reactions

The catalytic reactions are carried out in a microflow, fixed-bed reactor at atmospheric pressure with 500 mg of catalyst. Prior to reaction the catalysts are generally dried for 1 h in flowing Ar and reduced in flowing H₂ for 2 h at 500°C. At this point either the sample is sulfided at 500°C for 17 h with 9.4 ppm H₂S in H₂ (ratio of total sulfur to surface metal ca. 2) or, if sulfur was not added, this step involved pure H₂ only. The sample is then cooled to the reaction temperature of 400°C in flowing Ar and purged in flowing H₂ for 1 h. The reaction feed is composed of a mixture of H₂ and *n*-hexane (*n*C₆) in a ratio of 9 to 1, and the flow rate is 120 ml/min. The reaction products are analyzed by a Hewlett-Packard 5790A GC with a ¼-in. column packed with Porapak Q.

A reaction profile for sulfided and unsulfided PtRe/Al₂O₃ is shown in Fig. 1. This type of profile is typical for all catalysts studied in the respect that steady state appears to be achieved at 20 h time on stream. Results for this, and all other catalysts, are reported in Table 2 in terms of moles of *n*C₆ converted. For clarity, all products with less than six carbon atoms are grouped together as hydrogenolysis/cracking products (C₆-), all C₆ molecules, with the exception of benzene and *n*-hexane, are categorized as isomerization products (isomers), and "aromatics" represents benzene. The quantities reported as "initial" were taken at 5 min time on stream, "steady state" values were taken at 20.5 h time on stream.

B3. Oxidation of Carbonaceous Overlayers

After the catalytic reaction has been followed for 20.5 h, the sample is cooled to

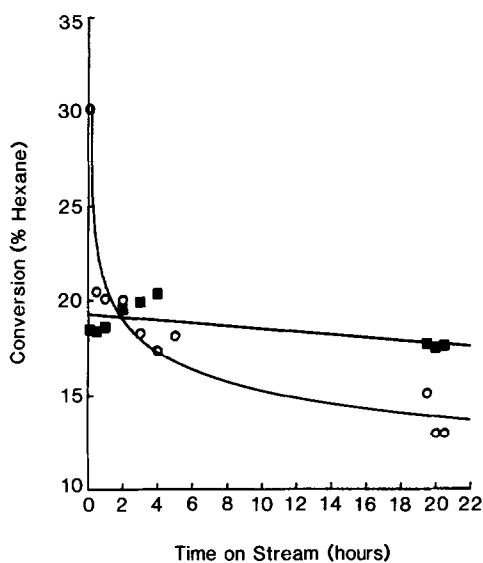


FIG. 1. Hexane conversion (% hexane converted) vs time on stream (h) for PtRe/Al₂O₃ (○) and PtRe(S)/Al₂O₃ (■). Temperature = 400°C; total pressure = 1 atm; H₂/*n*C₆ = 9.

room temperature in a flow of Ar. It is then sealed in the Ar atmosphere with Teflon valves, before transfer to the apparatus represented schematically in Fig. 2. This is a flow system in which carbon and hydrogen burn-off can be monitored in a temperature-programmed manner (temperature ramp = 8°C/min) by a dedicated mass spectrometer. Moisture is removed from the reactor dead volume by several purge and evacuate steps before the valves isolating the catalyst are opened. The samples are oxidized in a 60 ml/min flow of 5% O₂ in He. The gas flow downstream of the reactor is split off such that about one-half of the gas continues on to vent. The remainder of the gas passes into a three-stage pressure reduction system. This consists of a metering valve that regulates flow into a capillary tube which is pumped down by a mechanical pump. The mass spectrometer continuously samples the gas mixture from the capillary tubing through a variable leak valve. The mass spectrometer is pumped with an oil diffusion pump and operates at about 10⁻⁶ Torr. Liquid N₂ traps are placed at the

TABLE 2
Reaction Data

Catalyst	S (Y/N)	Activity <i>n</i> -hexane conversion (% converted)	Molar Selectivities (% product)		
			C ₆	Isomers	Aromatics
Pt/SiO ₂	N				
Initial		17.6	24.0	55.5	20.5
Steady state		6.9	31.7	46.3	22.0
Re/SiO ₂	N				
Initial		5.6	100.	0	0
Steady state		2.1	100.	0	0
Re/Al ₂ O ₃	N				
Initial		9.5	91.6	0	8.4
Steady state		3.8	100.	0	0
Pt/Al ₂ O ₃	N				
Initial		20.7	39.0	38.6	22.4
Steady state		11.8	41.4	40.6	18.0
	Y				
Initial		20.1	25.6	70.7	3.7
Steady state		11.0	36.7	53.1	10.2
PtRe/Al ₂ O ₃	N				
Initial		30.2	41.4	33.0	25.9
Steady state		13.0	33.9	37.1	29.0
	Y				
Initial		18.5	13.9	85.0	1.6
Steady state		17.7	23.3	73.5	3.6
Pt/Al ₂ O ₃ -Cl	N				
Initial		63.6	62.6	24.9	12.5
Steady state		37.1	58.1	33.6	8.3
	Y				
Initial		26.2	13.1	81.3	5.6
Steady state		18.8	29.0	62.2	8.8
PtRe/Al ₂ O ₃ -Cl	N				
Initial		43.1	27.2	41.8	31.1
Steady state		22.9	21.9	60.0	18.1
	Y				
Initial		33.4	19.6	77.7	2.7
Steady state		33.1	14.4	80.0	5.6
PtRe/Al ₂ O ₃ (SI)	N		No pretreatment		
Initial		39.2	62.1	34.7	12.1
Steady state		15.0	41.4	47.3	11.3
	Y				
Initial		13.5	17.6	82.4	0
Steady state		20.4	21.5	76.1	2.4
PtRe/Al ₂ O ₃ (SI)	N		Ar; 500°C		
Initial		23.8	38.8	41.0	20.2
Steady state		13.3	30.8	56.1	13.1
	Y				
Initial		9.5	17.2	82.8	0
Steady state		21.4	25.3	72.6	2.1

Note. Catalyst 0.5 g; flow rate = 120 ml/min; H₂/*n*C₆ = 9; temperature = 400°C.

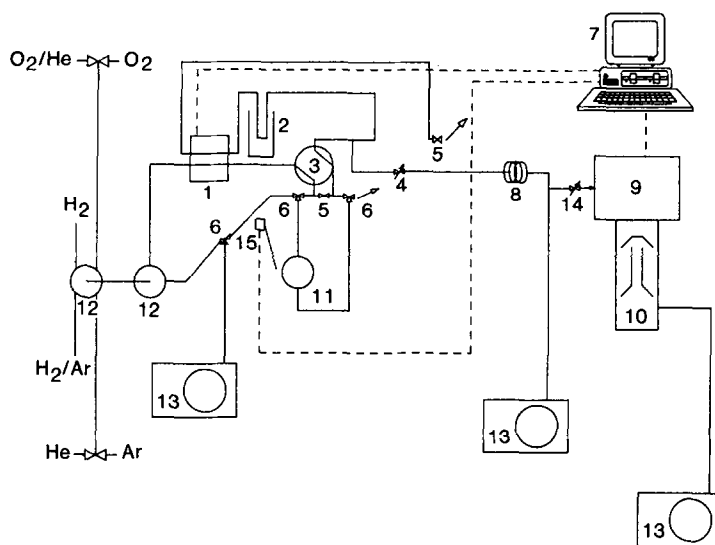


FIG. 2. Schematic representation of equipment used in temperature-programmed studies. Solid lines represent gas flow directions; dashed lines represent electrical connections. Designations: 1, thermal conductivity detector (TCD); 2, molecular sieve trap; 3, 4-way valve; 4, metering valve; 5, bellows on/off valve; 6, 3-way valve; 7, personal computer; 8, capillary tube; 9, mass spectrometer; 10, oil diffusion pump; 11, reactor; 12, 5-way valve; 13, mechanical pump; 14, variable leak valve; 15, thermocouple.

vacuum side of each mechanical pump and at the high-vacuum side of the oil diffusion pump to minimize oil backstreaming. The mass spectrometer and the temperature programmer are interfaced to a personal computer for data acquisition.

The decrease in oxygen partial pressure and evolution of CO_2 are recorded every 6 s. A burn-off profile for unsulfided PtRe/ Al_2O_3 after a reaction is displayed in Fig. 3. It can be seen that the decline in O_2 concentration reflects CO_2 evolution rather well. The number of moles of O_2 consumed is always greater than the moles of CO_2 produced, due to oxidation of both metals, hydrogen in the carbonaceous layer, and sulfur (when applicable). It was determined from subsequent temperature-programmed reduction that Pt was oxidized to 4+ and Re was oxidized to 7+ during the above oxidation treatment. To account for sulfur oxidation we assume that after a reaction, S/Re is 1, for PtRe catalysts, and S/Pt is 0.5 for Pt catalysts. These estimates are proba-

bly high, since neither SO_2 nor SO_3 is detected during burn-off. If lower estimates are made for the S/M ratios, the H/C ratios for the overlayers on the sulfided catalysts become accordingly higher. The difference in total O_2 consumed and that necessary to oxidize carbon, sulfur, and the metals is assigned to O_2 involved in oxidation of surface hydrogen to water. The quantitative values of both carbon and hydrogen retained on the catalyst after each reaction are reported in Table 3.

C. RESULTS AND DISCUSSION

C1. Peak Characterization

The oxidation of carbonaceous deposits on Pt/NaY (Fig. 4, Trace A) gives one CO_2 peak with a maximum at 180°C . The location of this peak correlates well with that ascribed to carbon oxidation on Pt metal by Barbier *et al.* (17). This peak appears to be very well defined, and, consequently, we have tried to fit it with a mathematical ex-

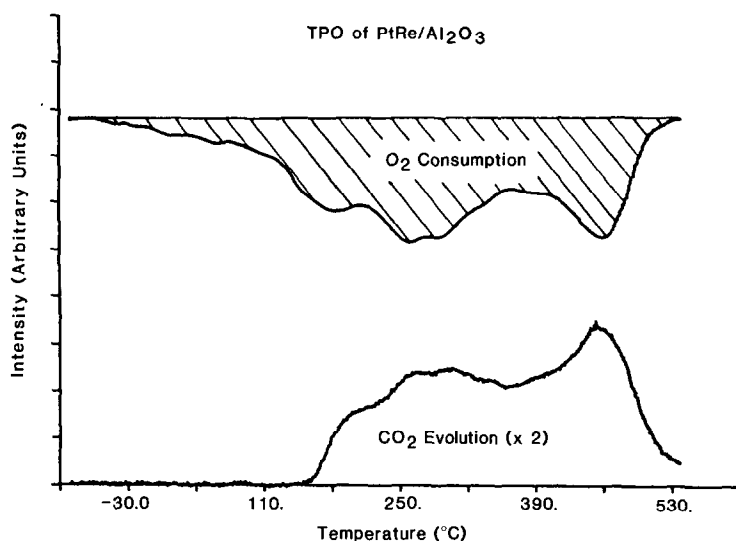


FIG. 3. Variation in CO_2 and O_2 concentration during temperature-programmed oxidation of carbon and hydrogen over aged $\text{PtRe}/\text{Al}_2\text{O}_3$ (intensity is in arbitrary, but comparable units).

pression making use of a least-squares method of fit. An approximation of a Gaussian curve (dashed line) gives a very good fit with a correlation coefficient of 0.990 and an average variance of 2.98×10^{-3} . The curve can also be fit to a power law (Fig. 4, Trace B), for which we have assumed pseudo-zero-order kinetics in O_2 . The best

fit is obtained when the order in C is 1.5. In this case, the correlation coefficient is 0.983 and the average variance is 4.84×10^{-3} . From this fit, the activation energy for the carbon oxidation is calculated to be 16 kcal mol^{-1} with a preexponential factor of $5.69 \times 10^{11} \text{ mol}^{-0.5} \text{ s}^{-1}$.

When Pt is supported on SiO_2 , the detec-

TABLE 3
Carbon and Hydrogen Retained on Catalysts

Catalyst	S (Y/N)	Carbon retained ($\mu\text{mol/g-cat}$)	Hydrogen retained ($\mu\text{mol/g-cat}$)	C/M	H/C
Re/ SiO_2	N	ND	ND	—	—
Pt/ SiO_2	N	28.1	60.4	1.1	2.15
Re/ Al_2O_3	N	118	62.2	11.0	0.53
Pt/ Al_2O_3	N	354	128	19.7	0.36
	Y	226	344	12.6	1.52
PtRe/ Al_2O_3	N	216	51.4	7.5	0.24
	Y	99.0	182	3.5	1.84
Pt/ $\text{Al}_2\text{O}_3\text{-Cl}$	N	342	126	9.4	0.37
	Y	224	174	6.2	0.78
PtRe/ $\text{Al}_2\text{O}_3\text{-Cl}$	N	200	101	4.6	0.51
	Y	116	185	2.7	1.59
PtRe/ $\text{Al}_2\text{O}_3(\text{SI})$, no pretreatment	N	163	39.2	5.2	0.24
	Y	114	96.8	3.7	0.85
PtRe/ $\text{Al}_2\text{O}_3(\text{SI})$, Ar; 500°C	N	234	72.8	7.5	0.31
	Y	104	63.2	3.3	0.61

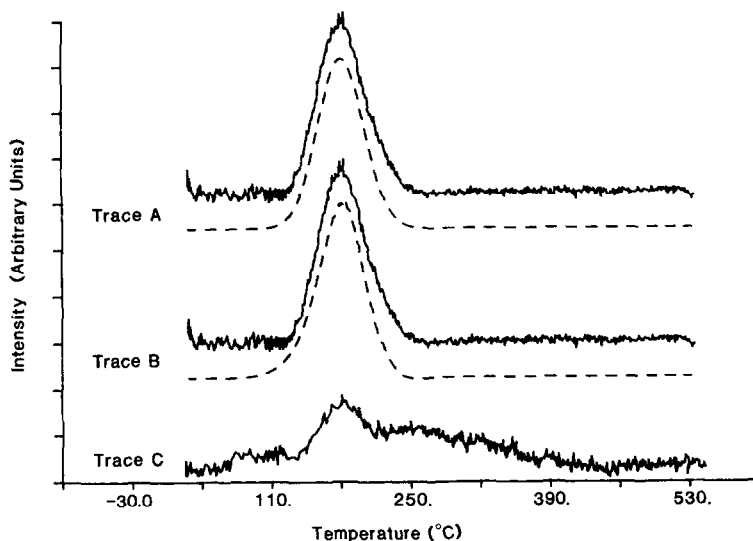


FIG. 4. CO₂ evolution during temperature-programmed oxidation of Pt/NaY and Pt/SiO₂ catalysts. Trace A is Pt/NaY fit with Gaussian approximation; Trace B is Pt/NaY fit with power law; Trace C is Pt/SiO₂ (intensity is in arbitrary, but comparable units).

tion limit of the apparatus is being approached (.03 wt% carbon), and a poor spectrum results (Fig. 4, Trace C). Nevertheless, at least two separate peaks are clearly discerned at 180 and 250°C. For Pt/ γ -Al₂O₃ the peaks are no longer well resolved (Fig. 5, Trace A). If a Gaussian peak

shape is still assumed, then the CO₂ profile can be fit with three peaks. The low-temperature peak is again assigned to Pt-catalyzed oxidation of carbon located on the metal function, although now the peak maximum is at 285°C, and the activation energy of oxidation is calculated to be 19

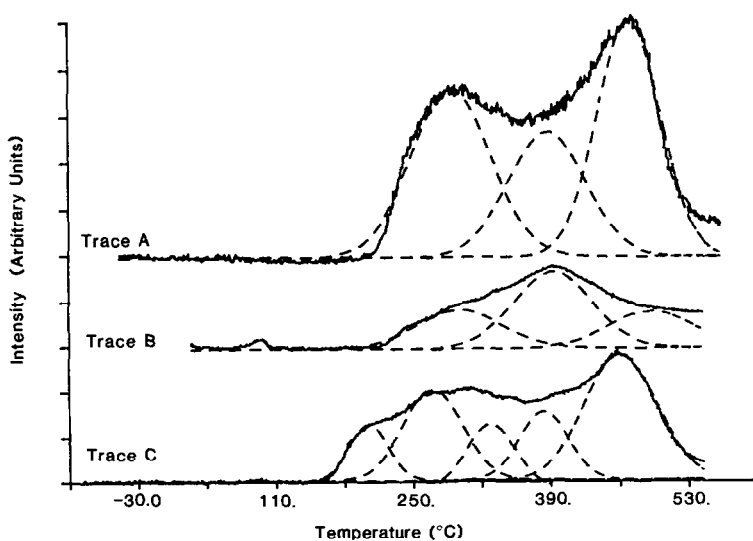


FIG. 5. CO₂ evolution during temperature-programmed oxidation of Pt/Al₂O₃ (Trace A), Re/Al₂O₃ (Trace B), and PtRe/Al₂O₃ (Trace C) (intensity is in arbitrary, but comparable units).

TABLE 4
Peak Assignments

Catalyst	S (Y/N)	Peak number temperature (°C) [area (μmol/g-cat)]				
		1	2	3	4	5
Pt/SiO ₂	N	180 [12.0]	250 [16.1]	—	—	—
Re/Al ₂ O ₃	N	—	—	290 [30.7]	390 [56.3]	485 [31.2]
Pt/Al ₂ O ₃	N	—	285 [124]	—	380 [89.2]	465 [140]
	Y	210 [5.1]	275 [79.0]	—	365 [59.2]	460 [82.4]
PtRe/Al ₂ O ₃	N	200 [20.6]	265 [50.4]	325 [29.6]	380 [31.6]	455 [84.2]
	Y	200 [16.4]	265 [25.4]	320 [7.9]	370 [16.8]	450 [32.2]
Pt/Al ₂ O ₃ -Cl	N	195 [21.8]	260 [27.4]	—	360 [105]	450 [188]
	Y	185 [16.0]	225 [8.8]	—	345 [104]	455 [92.2]
PtRe/Al ₂ O ₃ -Cl	N	190 [22.2]	240 [10.7]	300 [31.0]	375 [49.8]	455 [86.2]
	Y	195 [31.2]	230 [10.0]	295 [20.0]	365 [16.2]	440 [38.9]
Pt/NaY	N	180 [43.0]	—	—	—	—

kcal mol⁻¹. The other peaks, at 380 and 465°C with E_a 's of 27 and 41 kcal mol⁻¹, respectively, occur at temperatures typical for oxidation of carbon located on acidic metal oxide supports (17, 45).

The CO₂ profile for Re/γ-Al₂O₃ can also be deconvoluted into three separate peaks (Fig. 5, Trace B). The two associated with alumina are present at 390 and 485°C. The first peak (290°C) is now assigned to carbon interacting with Re. The temperature-programmed oxidation profile of the PtRe/Al₂O₃ catalyst is composed of five individual peaks (Fig. 5, Trace C). The early two are typical for carbon located on Pt (200 and 265°C), and the last two resemble oxidation of carbon on alumina (380 and 455°C). The middle peak (325°C) is found only when Re is present, so we ascribe this peak to oxidation of carbon located there.

In conclusion, the approximation of the data with a Gaussian function proves satisfactory. Consequently we have used this technique to analyze the CO₂ profiles for most of the catalysts studied. These peak assignments, including peak locations and integrated peak areas, are listed in Table 4.

C2. Sites Responsible for Carbonaceous Layer Deposition

Before proceeding further in the present study, it is important to identify whether the support or the metal is of primary importance in the formation of carbonaceous overlayers under the particular reaction conditions utilized. The metal function was first isolated by impregnation and reduction onto a very slightly acidic SiO₂ support. The reaction results for both Pt/SiO₂ and Re/SiO₂ in Table 2 show a rather pro-

nounced deactivation from initial to steady state. Re catalyzes only the hydrogenolysis, while Pt gives the entire spectrum of products. The ensuing oxidation of these samples shows very little carbon oxidation; only 28.1 μmol carbon was retained on Pt, and the amount of carbon on Re was below detection limits (Table 3). The H/C ratio of the residue remaining on Pt was 2.15. This is rather high and is typical for C residing on the metal function (10).

Supporting these metals on nonchlorided $\gamma\text{-Al}_2\text{O}_3$ does not alter the activity of Pt appreciably, but increases the activity for the Re catalyst (Table 2). The amount of carbon retained on these catalysts is significantly higher, however; Pt/ Al_2O_3 contains 354 $\mu\text{mol/g-cat}$ (12.6 times more than that on Pt/ SiO_2), and Re/ Al_2O_3 contains 118 $\mu\text{mol/g-cat}$. Although most of this carbon is located on the support (Table 4), the carbon located on the metal function is also increased relative to the metals supported on SiO_2 . The carbonaceous deposits on the alumina-supported catalysts also have a low H/C ratio, which is very typical of coke formed on acid sites.

From these results, it seems difficult to assign a large amount of coking activity to the metal function. It is reasonable to conclude that for the current reaction conditions used, coke formation predominantly occurs on the support, and the metal function may be responsible for hydrogenating deposited carbon and extending the active life of acidic metal oxides (23).

C3. Pt/ Al_2O_3 and PtRe/ Al_2O_3 : the Effect of Coimpregnation

The dependences of catalyst activities on time on stream are very similar for the non-sulfided samples. Therefore, characterization by two numbers in Table 2, viz. initial and steady-state activity, in combination with one representative curve in Fig. 1, thus provides an adequate description of each sample. More extensive time-on-stream curves up to 100 h at atmospheric and elevated pressures were given in Refs.

(15, 16). While the main purpose of Table 2 is to compare different samples that were tested under identical conditions, caution should be taken in comparing them with literature data. As one referee reminded us, the first data point for PtRe in Kluksdahl's patent was taken after 48 h on stream. Catalyst deactivation in the initial stage, as described in the present paper, is thus ignored in many patents.

Table 2 shows in accordance with previous observations (16, 25) that Re addition to Pt/ Al_2O_3 increases the initial activity of the catalyst. In addition, the deactivation of the PtRe catalyst is more pronounced; the steady-state activity is decreased from the initial by 57% for PtRe and 43% for Pt. It is also interesting that Re increases both the initial and the steady-state yield of benzene. This has also been observed previously (26) and is a clear indication of the effect of Re upon the dehydrocyclization activity of the catalyst.

It can be seen from both the CO_2 profile and Table 4 that, even though the degree of deactivation is greater when Re is present, the amount of carbon retained on both the metal and the support is lowered relative to the monometallic Pt catalyst. This is supported by observations by other authors who have attributed the lower coke levels to a high (de)hydrogenation activity due to the presence of Re (18, 27, 28). Yet, even though the amount of C retained on the sample is decreased by 39%, the results listed in Table 3 show that Re does not change the H/C ratio of the carbonaceous layer appreciably.

It is well established that for catalyst preparations similar to those used in this study, Re interacts with both Pt (4, 25) and $\gamma\text{-Al}_2\text{O}_3$ (5, 29–32). The interaction with the support is most likely through exposed Al^{3+} ions, thus poisoning the coke-producing Lewis acid sites (20). It is difficult to understand, however, how less coke on the catalyst leads to greater deactivation. Apparently, the coke produced on the metal is a more selective poison than that which is

produced on Pt/Al₂O₃. As stated above, the interaction of Re with Pt increases the aromatization activity of the catalyst. A speculation at this point is that the carbon remaining on the metal function may also have a higher percentage of *sp*² character than that on the monometallic Pt catalyst, thus resembling two-dimensional polymeric graphite more than *sp*³ carbon. Obviously, this phenomenon requires further study.

C4. The Effect of Sulfur

It is well documented that sulfur decreases the initial activity, but enhances the stability against deactivation of reforming catalysts. This beneficial effect is greater for PtRe/Al₂O₃ than for Pt/Al₂O₃ (7, 15, 16, 27, 33, 34). Our results (Table 2) agree completely with these reports. After presulfidation, PtRe deactivates only 5% during 20.5 h time on stream, whereas Pt deactivates 57%. Sulfur also increases the selectivity for isomerization at the expense of both hydrogenolysis and aromatization. Yet the selectivities of the latter increase with time, indicating that sulfur is stripped from the catalyst as the reaction progresses.

Results in Table 3 show that presulfiding has a profound effect on both the quantity and the quality of the carbonaceous overlayer formed during *n*C₆ conversion reactions, and, as expected, these effects are greater for bimetallic samples than for Pt monometallic catalysts. Carbon accumulation is decreased 54% for PtRe and 36% for Pt in the presence of sulfur; both the metal and the support retain less carbon (Table 4). The carbonaceous layer is also much richer in hydrogen over the sulfided catalyst (Table 3), with H/C ratios increasing from 0.24 to 1.84 and 0.36 to 1.52 for PtRe and Pt, respectively. As stated above, these numbers are calculated based on rather conservative assumptions regarding oxygen consumption by chemisorbed sulfur; in reality the H/C ratio for the sulfided samples may be higher.

Sulfur thus reduces the amount of coke

deposited and makes this coke "softer," i.e., more hydrogen rich. A number of causes might be considered for this. Sulfur can interact with Lewis acid sites (35–37) and thus deactivate sites for coking. This phenomenon fails, however, to explain the marked differences which sulfur exerts on activity and selectivity of different Al₂O₃-supported metal catalysts (16). More relevant is the interaction of sulfur with the metal function (38); it decreases the average size of metallic surface ensembles, as is manifest from the changes in selectivity, and it thus lowers the coking rate on the metal (16, 39). Consequently, the hydrogenation ability is better preserved, and coke precursors are more efficiently volatilized on both the metal and the support.

The steep initial activity decline of sulfur-free PtRe in comparison to the presulfided catalyst suggests that much of the coke deposition on the former takes place in the first few hours; this carbon is possibly carbidic. It would be wrong, however, to conclude that the effects of sulfur were limited to this initial stage, or that the steady-state performances of presulfided and carbided PtRe catalysts were similar. Such hypotheses are contradicted by the vastly different selectivities after 22 h (see Table 2) and by the results of the 100-h tests at 1.5 MPa (see Ref. 16, Fig. 5). That test clearly showed that PtRe/Al₂O₃ maintained a perfectly constant activity, when exposed to a feed containing 1 ppm of H₂S, whereas the activity of the same catalyst continued to decline in the absence of sulfur. This test also revealed that the activity of Pt/Al₂O₃ decreased with time even in the presence of 1 ppm of H₂S. Only the combination of platinum with rhenium and sulfur shows perfect activity maintenance (16).

As stated in the Introduction, the present research is primarily focused on the effect of sulfur on the H/C ratio of the deposited coke. The present results show that this ratio is significantly higher for the presulfided than for the nonpresulfided PtRe samples in full accordance with the assumption that re-

organization of adsorbed fragments to polymeric or graphitic entities is impeded by chemisorbed sulfur. This effect of adsorbed sulfur is greater for PtRe than for Pt due to the fact that sulfur interacts more strongly with Re than with Pt atoms. Previously we had demonstrated that mixed PtRe particles are abundantly in our samples after reduction (25). Adsorbed S atoms are likely to be more immobile on Re than on Pt atoms and, therefore, more efficient obstacles to the reorganization of carbonaceous species.

C5. The Effect of Pt and Re Interaction

It has been previously demonstrated that deep hydrogenolysis to methane is an effective probe reaction for detecting mixed PtRe ensembles in supported, highly dispersed catalysts (4, 25). For the particular sample prepared by successive impregnation, this probe had shown that, after drying at high temperatures prior to reduction, little interaction of Re with Pt was noted in the reduced catalyst, but this interaction was pronounced if the catalyst was directly reduced with no prior drying step (5).

The present work shows, again, that a drying step before reduction has a significant effect on the activity of the catalyst, particularly for hydrogenolysis (Table 2). When the catalyst was directly reduced the conversion was 39.2%, but, if it had been heated first, the conversion was only 23.8%. This change in activity can be totally accounted for by an increase in the rate of hydrogenolysis; the yields of isomers and benzene were relatively unchanged. There was also a fourfold increase in the methane yield of the directly reduced catalyst relative to that severely dried. While we had observed this before, the new finding is that a large extent of Pt and Re interaction results in a more pronounced activity decline. The sample, with higher PtRe interaction, deactivated by 62%, while the predried sample suffered only a 44% drop in activity.

Even though the latter sample deacti-

vates less, it retains 44% more carbon than the sample which was directly reduced (Table 3). The H/C ratios are very similar for both samples. In this case, as before in the comparison of nonsulfided Pt/Al₂O₃ and PtRe/Al₂O₃, the extent of deactivation cannot simply be correlated to the quantity of carbon deposited or the H/C ratio.

There are more apparent similarities in the catalysis of the two samples after presulfiding; the activities and selectivities are almost identical (Table 2). Yet the activities of both catalysts increase significantly with time on stream, probably due to sulfur removal from the surface under reaction conditions. As demonstrated above with the other catalysts, S is a selective poison, having a greater effect on the hydrogenolysis activity of the catalyst. The production of methane is particularly attenuated, decreasing by a factor of 223 for the nondried sample and 116 for the dried one. Also, in both cases, there is no apparent activity for aromatization initially, but this activity increases with time on stream.

The similarities seen in the catalytic behavior carry over to the temperature-programmed oxidation as well. Essentially the same amount of carbon accumulated on both these samples during the conversion experiments (Table 3). The CO₂ profiles in Fig. 6 show, however, that the distributions of this carbon are somewhat different for these two cases. When the catalyst was directly reduced, a large majority of the Re interacted with Pt (5), and carbon was evenly distributed between the support and the metal. After a severe prereluction drying temperature, Re interacted more strongly with the support (5, 29–32), less carbon remained on the metal, and more was on the support than in the former situation. The H/C ratios also seemed to be higher for the catalyst which was directly reduced (Table 3). This may result from the larger interaction of Re with Pt, allowing sulfur to more effectively block reorganization of carbonaceous fragments into graphitic entities on the metal clusters. Or it

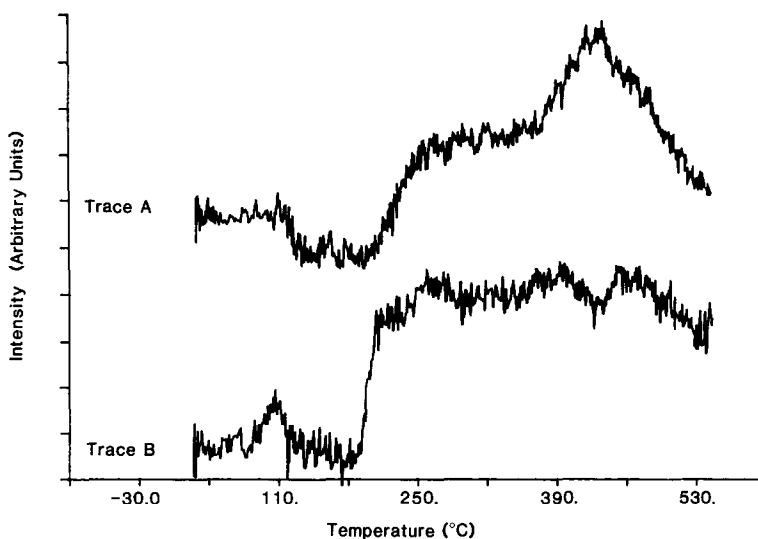


FIG. 6. CO₂ evolution during temperature-programmed oxidation of PtRe/Al₂O₃(SI) reduced after 500°C drying step (Trace A), and PtRe/Al₂O₃(SI) directly reduced (Trace B) (intensity is in arbitrary, but comparable units).

may simply be due to the greater amount of carbon located on the metal, which tends to retain more hydrogen than carbon residing on the support (10).

C6. The Effect of Cl⁻

Chloride is an essential component of reforming catalysts; therefore its effect on coking should be investigated. It is important to note that, in addition to greatly increasing the Brønsted acidity, many studies indicate that Cl⁻ influences the metal function as well (40–43); thus, the presence of Cl⁻ will most likely affect coking on both metal and support.

It can be seen from the catalytic results listed in Table 2 that the chloride-containing samples display a higher activity than those supported on pure alumina. The increase in activity is mainly due to enhanced isomerization or cracking activity, and little difference is observed in the benzene yield. The chlorided catalysts also display better activity maintenance, both in the presence of sulfur and in its absence, than do the nonchlorided samples.

The CO₂ profiles for the oxidation of car-

bon on both Pt/Al₂O₃-Cl and PtRe/Al₂O₃-Cl are represented in Fig. 7. The overall shapes of the profiles agree qualitatively with those previously reported in the literature (10, 20). Deconvolution shows that, with the exception of the additional 190°C peak for Pt/Al₂O₃-Cl, the number of peaks and their positions are generally the same as those for the nonchlorided counterparts. In addition, the quantitative evaluations of the carbon burn-off presented in Tables 3 and 4 show that all the trends observed for the nonchlorided catalysts with the addition of Re and S are also valid for these samples.

Chloriding has no observable effect on the amount of carbon retained on the catalysts in these experiments (Table 3). Consequently, it is difficult to attribute coke formation to the presence of Brønsted acidity, but Lewis acidity seems more important (20). The chloride does seem to affect the distribution of the coke, however; a greater percentage of carbon remains on the support, while less moves to the metal function (Table 4). Presumably Brønsted acidity affects the mobility of carbonaceous residues, causing them to remain on the sup-

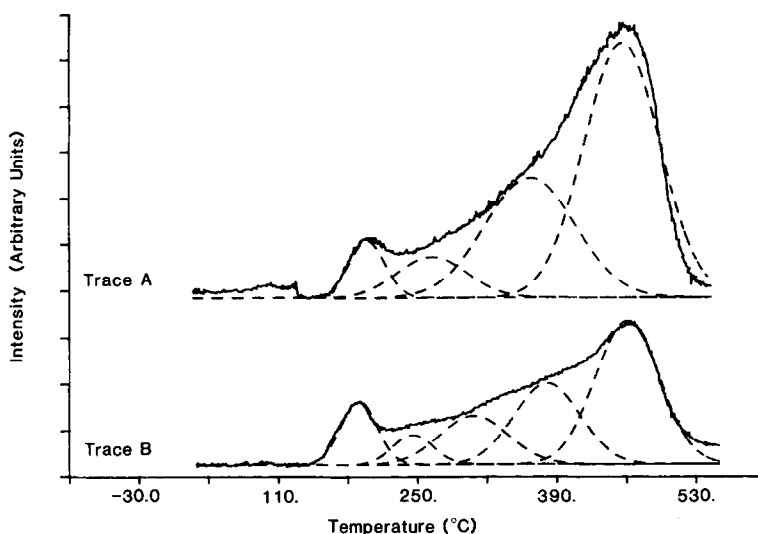


FIG. 7. CO₂ evolution during temperature-programmed oxidation of Pt/Al₂O₃-Cl (Trace A) and PtRe/Al₂O₃-Cl (Trace B) (intensity is in arbitrary, but comparable units).

port rather than move to the metal. This may also explain the increased steady-state activity of these catalysts relative to those supported on pure alumina, for the vitality of the metal function appears to be the decisive factor in whether a bifunctional catalyst will or will not deactivate (44).

D. CONCLUSIONS

Under the conditions of our test reaction coke is formed at Lewis acid sites of partially dehydroxylated γ -Al₂O₃. Less carbon is deposited on Pt/SiO₂ than on Pt/Al₂O₃. Chlorine affects the distribution of carbon over metal and support, possibly because Brønsted sites reduce surface mobility of coke precursors.

Re decreases the quantity of carbonaceous residues, and, as more Re interacts with Pt, less carbon is deposited on the catalyst. However, in the absence of S, PtRe catalysts undergo a more pronounced deactivation which increases with increasing PtRe interaction. Therefore, no simple correlation between catalyst deactivation and overall carbon deposition is proposed.

When Re and S are combined, activity maintenance is enhanced and carbon depo-

sition is lower. Catalytic activity decreases little. In fact, for some samples it actually increases with time, possibly due to some sulfur stripping. The effect of sulfur on carbon attenuation is larger by 15–25% for PtRe relative to a monometallic Pt catalyst.

The most dramatic effect of sulfiding these catalysts is the very marked increase in the H/C ratio for the carbonaceous deposits. In every case sulfur strongly affects the nature of carbon retained by allowing it to better hold on to hydrogen, and, consequently, it is less graphitic and less harmful to activity. Not only does adsorbed sulfur change the nature of coke in the initial stage of the catalyst performance but also the more permanent effects of sulfur adsorbed on PtRe particles are manifest from the pronounced changes in selectivity, which persist until the end of the 22-h test. In previous tests at high pressures and 100 h run time, a permanent effect of 1 ppm of H₂S in the feed on the activity and selectivity maintenance of PtRe/ γ -Al₂O₃ had been demonstrated.

Another effect upon the H/C ratio is the extent of PtRe interaction. When this interaction is increased, and S is added, the H/C

ratio is detectably higher than in the case where the Pt and Re interaction is inhibited. This adjusted interaction also plays a role in the carbon distribution over the catalyst.

These results can, for the most part, be explained by the model proposed previously (7, 8) and summarized in the Introduction to the present paper. One of its basic assumptions, viz. that PtRe bimetallic particles are formed on these catalysts, has since been established by separate results (25). A second assumption, that sulfur, which is strongly adsorbed on Re, subdivides the surface of the bimetallic PtRe clusters into smaller ensembles of bare Pt atoms and thus lowers the activity for hydrogenolysis, has also been confirmed experimentally. The third assumption that graphitization of the initial hydrocarbonaceous deposit is suppressed on PtRe-S surfaces seems to be supported by the present data. Coke formation appears to be a structure-sensitive reaction (14, 36, 44) possibly including thorough reconstruction of the initial hydrocarbonaceous deposit. If so, it is not unreasonable to conclude from the large H/C ratios in carbonaceous deposits observed after sulfidation that chemisorbed sulfur inhibits the reorganization of these initial deposits into deleterious pseudo-graphitic overlayers.

REFERENCES

1. Kluksdahl, H. E., U.S. Patent 3,415,737 (1968).
2. Bertolacini, R. J., and Pellet, R. J., in "Catalyst Deactivation" (B. Delmon and G. F. Froment, Eds.), p. 73. Elsevier, Amsterdam, 1980.
3. Bolivar, C., Charcosset, H., Fretty, R., Primet, M., Tournayan, L., Betizeau, C., Leclerq, G., and Maurel, L., *J. Catal.* **39**, 249 (1975).
4. Augustine, S. M., and Sachtler, W. M. H., *J. Phys. Chem.* **91**, 5953 (1987).
5. Augustine, S. M., and Sachtler, W. M. H., *J. Catal.*, in press.
6. Haining, I. H. B., Kembal, C., and Whan, D. A., *J. Chem. Res.*, 2056 (1977); 364 (1978).
7. Biloen, P., Helle, J. N., Verbeek, H., Dautzenberg, F. M., and Sachtler, W. M. H., *J. Catal.* **63**, 112 (1980).
8. Sachtler, W. M. H., *J. Mol. Catal.* **25**, 1 (1984).
9. Somorjai, G. A., and Blakeley, D. W., *Nature (London)* **258**, 580 (1975); Blakeley, D. W., and Somorjai, G. A., *J. Catal.* **42**, 181 (1976).
10. Lankhorst, P. P., de Jongste, H. C., and Ponec, V., in "Catalyst Deactivation" (B. Delmon and G. F. Froment, Eds), p. 43. Elsevier, Amsterdam, 1980.
11. Barbier, J., in "Catalyst Deactivation 1987" (B. Delmon and G. F. Froment, Eds), p. 1. Elsevier, Amsterdam, 1987.
12. Gardner, N. C., and Hansen, R. S., *J. Phys. Chem.* **74**, 3298 (1970).
13. Thomson, S. J., and Webb, G., *J. Chem. Soc. Chem. Commun.*, 526 (1976).
14. Davis, S. M., Zaera, F., and Somorjai G. A., *J. Catal.* **77**, 439 (1982).
15. Shum, V. K., Butt, J. B., and Sachtler, W. M. H., *J. Catal.* **96**, 371 (1985).
16. Shum, V. K., Butt, J. B., and Sachtler, W. M. H., *J. Catal.* **99**, 126 (1986).
17. Barbier, J., Marecot, P., Martin, N., Elassal, L., and Maurel, R., in "Catalyst Deactivation" (B. Delmon and G. F. Froment, Eds), p. 53. Elsevier, Amsterdam, 1980.
18. Barbier, J., Corro, G., Zhang, Y., Bournville, J. P., and Franck, J. P., *Appl. Catal.* **16**, 169 (1985).
19. Barbier, J., and Marecot, P., *J. Catal.* **102**, 21 (1986).
20. Mieville, R. L., *J. Catal.* **100**, 482 (1986).
21. Parera, J. M., Verdone, R. J., Pieck, C. L., and Traffano, E. M., *Appl. Catal.* **23**, 15 (1986).
22. Lietz, G., Völter, J., Dobrovolszky, M., and Paál, Z., *Appl. Catal.* **13**, 77 (1987).
23. see Gates, B. C., Katzer, J. R., and Schuit, G. C. A., "Chemistry of Catalytic Processes." McGraw-Hill, New York, 1979.
24. Tzou, M. S., Jiang, H. J., and Sachtler W. M. H., *Appl. Catal.* **20**, 231 (1986).
25. Augustine, S. M., and Sachtler, W. M. H., *J. Catal.* **106**, 417 (1987).
26. Urbanovich, I. I., Gagarin, S. G., Gintovt, T. I., and Titova, L. I., *React. Kinet. Catal. Lett.* **27**, 59 (1985).
27. Coughlin, R. W., Kwakami, K., and Hasan, A., *J. Catal.* **88**, 150 (1988).
28. Margitfalvi, J., Göbölös, S., Kwaysser, E., Hege-dös, M., Nagy, F., and Koltai, L., *React. Kinet. Catal. Lett.* **24**, 315 (1984).
29. Kerkhof, F. P. J. M., Moullijn, J. A., and Thomas, R., *J. Catal.* **56**, 279 (1979).
30. Arnoldy, P., van Oers, E. M., Bruinsma, O. S. L., de Beer, V. H. J., and Moullijn, J. A., *J. Catal.* **93**, 231 (1985).
31. Edreva-Kardjieva, R. M., and Andreev, A. A., *J. Catal.* **94**, 97 (1985).
32. Hardcastle, F. D., Wachs, I. E., and Persans, P., personal communication.
33. Menon, P. G., and Prasad, J., "Proceedings, 6th International Congress on Catalysis, London, 1976" (G. C. Bond, P. B. Wells, and F. C. Tomkins, Eds.), Vol. 2, p. 1061. The Chemical Society, London, 1976.

34. Jossens, L. W., and Petersen, E. E., *J. Catal.* **76**, 273 (1982).
35. Deo, A. V., Dalla Lana, L. G., and Habgood, H. W., *J. Catal.* **21**, 270 (1971).
36. Lunsford, J. H., Zingery, L. W., and Rosynek, M. P., *J. Catal.* **38**, 179 (1975).
37. Rosynek, M. P., and Strey, F. L., *J. Catal.* **41**, 312 (1976).
38. Schay, Z., Matusek, K., and Guzzi, L., *Appl. Catal.* **10**, 173 (1984).
39. Clarke, J. K. A., *Chem. Rev.* **75**, 29 (1975).
40. Bournville, J. P., and Martino, G., in "Catalyst Deactivation" (B. Delmon and R. Froment, Eds.), p. 159. Elsevier, Amsterdam, 1980.
41. Sivasanker, S., Ramaswamy, A. V., and Ranasamy, P., *J. Catal.* **47**, 421 (1977).
42. Callender, W. L., and Miller, J. J., "Proceedings, 8th International Congress on Catalysis, Berlin, 1984," Vol. 2, p. 491. Dechema, Frankfurt am Main, 1984.
43. Augustine, S. M., Ph.D. thesis, Northwestern University, Evanston, IL, 1988.
44. Blakeley, D. W., and Somorjai, G. A., *J. Catal.* **42**, 181 (1976).
45. Magnoux, P., and Guisnet, M., *Appl. Catal.* **38**, 341 (1988).